Microwave analog to light scattering measurements on a fully characterized complex aggregate

Olivier Merchiers,[1] Jean-Michel Geffrin,[2] Rodolphe Vaillon,[1] Pierre Sabouroux,[2] and Bernard Lacroix[1]
[1]*Université de Lyon, CNRS, INSA-Lyon, UCBL, CETHIL, UMR5008, F-69621 Villeurbanne, France*
[2]*Institut Fresnel, Aix-Marseille Universités, Ecole Centrale Marseille, CNRS, Domaine universitaire de Saint Jérôme, 13392 Marseille, France*

(Received 27 March 2009; accepted 1 April 2009; published online 7 May 2009)

We present experimental measurements of three-dimensional electromagnetic wave scattering in the microwave frequency range, by a complex aggregate consisting of 74 primary spheres with fully known optical and geometrical properties. We measured the complete amplitude scattering matrix (or Jones matrix), from which the electric fields (amplitude and phase) with arbitrary polarization can be obtained. These results offer the opportunity to test approximate computational methods against experiments. © *2009 American Institute of Physics*. [DOI: 10.1063/1.3129196]

Microwave analogy principles have been applied since the 50s in order to analyze optical scattering properties of nonspherical particles and systems.[1] It has been shown that for an arbitrary fixed aggregate embedded in an infinite, homogeneous, linear, isotropic, and nonabsorbing medium, a dimensionless amplitude scattering matrix can be defined.[2] This property, known as the scale invariance rule, allows one to increase both object size (effective radius r) and incident wavelength (λ), keeping their size parameter $x=2\pi r/\lambda$ and complex refractive index constant, such that the scattering behavior of the analog object is identical to the original one. Since in the optical region, systems of interest are generally very small (from nanometers to micrometers in size), it is very difficult to control their refractive index, exact shape, and orientation and hence validate models. In the microwave region objects can be made macroscopic and consequently are easier to manufacture in a controlled fashion.

This scale translation was employed for the first time by Greenberg and later by Giese (see the review in Ref. 1). Both used a single wavelength (3.18 cm and 8 mm, respectively). This situation changed with the setup at the University of Florida.[3] Broadband (2.7–4 mm) and phase measurements became possible over a wide range of scattering angles (0°–168°). Nevertheless, some aspects still asked for improvements. The first one is the ability to make three-dimensional measurements, that is when emitter, target and receiver's exploratory displacements are not always in the same plane. The second one is the wavelength range. In the Florida facility, the operating wavelengths were still quite short. The measurements presented in this letter were realized at the anechoic chamber of the Institut Fresnel in Marseille (France).[4] This facility, as described later, provides solutions to the previously mentioned problems. Until now, studied objects were mainly, or regular particle arrays[5–7] or complex structures,[8–10] but of which the geometry was not always fully controlled. Hence for the last structures, strict comparison with computational results was still impossible. Furthermore, while the phase has been measured by Gustafson,[1] a thorough study of it and comparison with numerical results have never been presented. With the present study we try to fill in this gap. On the other hand, the obtained data will offer the possibility to the scientific community to directly test inversion algorithms since the target is perfectly known.

This letter is organized as follows. In the following section, we describe the experimental facility, we then explain briefly how we chose the microwave analogy parameters, the geometrical structure of the aggregate and its electric and magnetic properties. Next we describe how the aggregate was built and finally we present an insight of some of the most relevant results.

The following experiments were carried out by members of the Institut Fresnel in the anechoic chamber of the "Centre Commun de Ressources Microondes."[11] The main specificity of this equipment is the semicircular vertical arch which allows to measure fields almost all around the target under test (Fig. 1), especially outside of the target-receiver plane (called here the azimuthal plane). The system is based on a network analyzer (HP8510C) used with external mixers which allows to perform field measurements from a few gi-

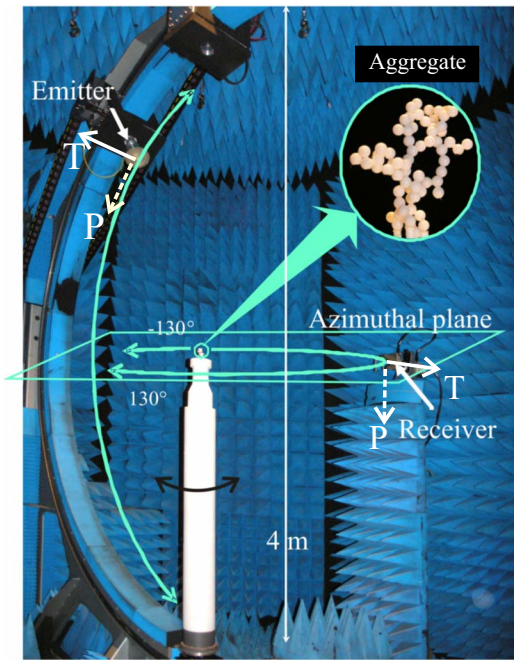

FIG. 1. (Color online) Experimental setup, polarization convention, and a close-up of the studied aggregate.

gahertz up to 20 GHz. The scattering measurements presented here required our cumulated knowledge and needed to improve performances of the system (the hardware, through shorting of the cables and the postprocessing software so as to compensate drift phenomena[12]) since the considered aggregate is the smallest target that we have ever measured with this equipment.

Choice of particle radius, dielectric properties, and geometrical structure, was originally guided by the analogy with soot particles. These particles can generally be modeled as fractal aggregates, to which the equation $N=k_0(R_g/a)^{D_f}$ can be applied where N, is the number of particles in the aggregate, k_0 is the prefactor, R_g is the gyration radius, a is the radius of the primary spheres, and D_f is the fractal dimension. We chose for the scale independent geometrical structure parameters the values: $N=74$, $D_f=1.7$, and $k_0=2$.[13] For the sake of simplicity and as a first attempt, we chose polyacetal, which has almost no absorption but does have a real part of the refractive index, very similar to soot.

To computationally generate such an aggregate we used a simple procedure which consists in sticking spheres in a random way but keeping only those combinations which fulfill $N=k_0(R_g/a)^{D_f}$.[14] Once we obtained the list of particles' coordinates,[13] we could start the actual building. Thereto we used a three-dimensional micromilling machine (Isel, Flatcom 20) that we arranged with specific tools to precisely manipulate spheres with 5.00 mm diameter. In order to make the simulation parameters as close as possible to the experimental situation, accurate knowledge of the geometrical structure of the aggregate and of its position with respect to the incident field is needed. Whereas the list of coordinates of spheres is precisely known from the computational generation and the building procedure, uncertainty on target's orientation was estimated of about 1°. As for spectral variation of the complex electric permittivity ε and magnetic permeability μ as a function of frequency, they were measured using the laboratory facility *EpsiMu* (Ref. 15) over the frequency interval [1-18] gigahertz. The refractive index is obtained from the formula $n+ik=(\varepsilon\mu)^{1/2}$. Since the experimental values do not show strong variations over this frequency interval, we used the mean values of real and imaginary parts of the refractive index, found to be equal to $1.78+i0.05$ with an estimated uncertainty of 5%.

The experimental setup described earlier allows the measurement of the so-called Jones matrix elements. We have to indicate that the measurements are made in a base which is different from Bohren and Huffman's.[16] Both conventions are related by two rotations. In our base, the Jones matrix becomes

$$\begin{pmatrix} E_S^T \\ E_S^P \end{pmatrix} = \begin{pmatrix} TT & TP \\ PT & PP \end{pmatrix} \begin{pmatrix} E_i^T \\ E_i^P \end{pmatrix}. \quad (1)$$

Details about the convention can be found in Ref. 17. Here, T stands for theta and P for phi. Since the matrix elements are complex values, they contain both amplitude and phase information. Experimental results were compared with solutions generated by Mackowski's T-matrix code for multiparticle clusters.[18] The following comparisons are a direct experimental validation of this and other codes.

The experimental results are presented in Figs. 2 and 3 where the absolute values and the phases of the four matrix elements are depicted. The represented data have been obtained for two different receiver-emitter configurations. In the first one both emitter and source are placed in the azimuthal plane. For the second one, the emitter was placed out of the azimuthal plane such that the propagation direction of the incident fields makes an angle of 30° with this plane without changing the aggregate position. We chose to present the results obtained with a frequency of the incident field of 16 GHz ($x_{\text{individual spheres}}=0.845$ and $x_{\text{aggregate}}=14.05$) since this is the computationally most demanding case we obtained from the measurements.

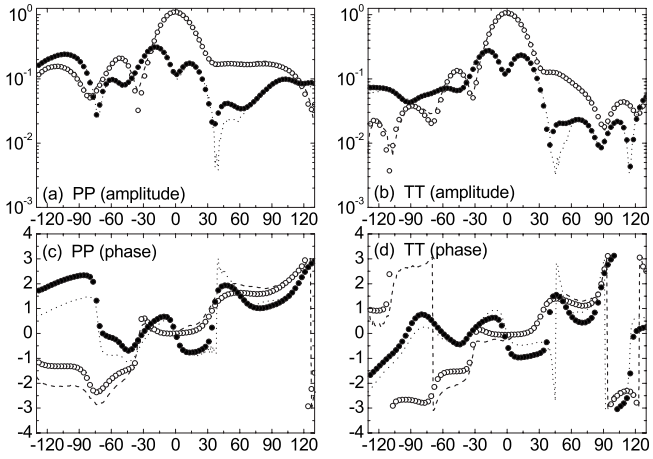

FIG. 2. Measurements and simulations obtained for the amplitudes [figures (a) and (b)] and phases [figures (c) and (d)] of the *PP* and *TT* matrix elements for the in and out of the azimuthal plane configurations as a function of the scattering angle in degrees (experimental data in plane: dashed line; simulated data in plane: white circles; experimental data out of plane: dotted line; simulated data out of plane: black circles).

As can be seen from Figs. 2(a), 2(b), 3(a), and 3(b), the amplitudes obtained with Mackowski's T-matrix code, compare very well to the experimental results. In order to obtain the overlap of both experimental and simulated data sets, we had to normalize them. Thereto we calculated the normalization constant C for the *PP* parameter and then applied it to *TT*, *TP*, and *PT* for both in and out of plane configurations.

For the cross terms *TP* and *PT*, the fit with the simulated results is not as good and especially for the region covering the scattering angles from −30° to 30°. For those off-diagonal matrix elements (cross polarization), as can be seen from Figs. 3(a) and 3(b), the amplitude level is one order of magnitude lower than for the co-terms and hence we have a

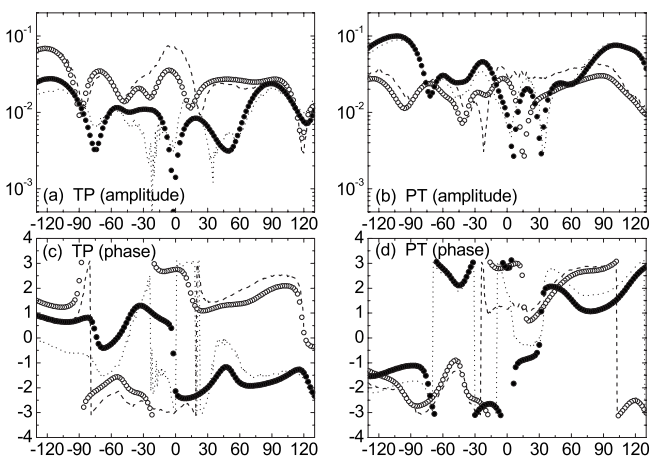

FIG. 3. Same as Fig. 2 but for the *TP* and *PT* matrix elements.

lower signal-to-noise ratio. On the other hand, for the measurement of *TP* and *PT*, polarizations of emitter and receiver have to be crossed. In the absence of a target, the detected field in the exact forward scattering direction should be identically zero. However, due to imperfections in the polarization control of emitter and receiver, this extinction is never total and hence residual energy is always present in the beam for those scattering directions.

The phases of matrix elements are represented in Figs. 2(c), 2(d), 3(c), and 3(d). In order to fit the experimental results with the model, a reference for the phases had to be set. We set the phase of *PP* to 0 (from now on we use for the phases of the parameters $i=PP$, *TT*, *TP*, *PT* the symbol ϕ_i) in the exact forward direction ($\theta_S=0°$) by subtracting from the phase for all scattering angles the value $\phi_{PP}(0°)$. We subtract then from all other ϕ_i's the same value $\phi_{PP}(0°)$. A good fit for the diagonal elements *PP* and *TT* is obtained. However, quality of it is not as good as for the amplitudes. While the shapes are well reproduced, the levels suffer more differences. This is mainly due to the really high sensitivity of the phase to the precise aggregate position in the experimental setup and its internal structure. Additional comments can be raised here. For both diagonal elements (*PP* and *TT*), the phase has a more or less step wise evolution with the scattering angle. For the interval $[-30°, 30°]$, a constant phase value is found. This corresponds to a low q value region ($q=\|\mathbf{k}_s-\mathbf{k}_i\|=2\pi\lambda^{-1}\sqrt{2(1-\cos(\theta_s))}$ is the amplitude of the scattering wavevector) for which the waves see a single particle. When q (in our case the scattering angle) is increased, the internal structure starts to be visible and a first phase delay appears and so on.

For the off-diagonal terms, the phase variation means that a phase lag appears between perpendicular polarization components. The incident linear polarization is changed to a general elliptic scattered polarization, which indicates the presence of anisotropy.

We now turn to the out of plane configuration. It has the advantage that the receiver suffers less from blinding by the source since both (receiver and emitter) are never on the same line of sight. However, the scattered signal is now slightly lower and hence the fits with the simulations are not as good as before. For the phase reference we took the value $\phi_{PP}(0°)$ for the out of plane measurement. Contrarily to the in plane measurements, the phases of *PP* and *TT* do not show such clear stepwise behavior as a function of the scattering angle. It should be noticed that the magnitude of the wavevector does not become zero in the exact forward scattering direction. This is expressed in the fact that the amplitudes of *PP* and *TT* do not show a coherent forward scattering lobe as was the case for the in plane measurements.

In summary, the four complex elements of the amplitude scattering matrix of an aggregate with fractal geometry consisting of 74 primary spheres were measured for different emitter-receiver configurations. The aggregate was built in a fully controlled way. Experimental results allow validating both approximate electromagnetic scattering codes and measurements applied to complex aggregates. We are currently extending this analysis to other orientations, frequencies, and working on enlarging the measurable scattering angle range (closer to backscattering). Furthermore we plan to build other aggregates with metallic particles and materials which show a higher absorption in the microwave region.

The authors would like to thank the ANR (Agence Nationale de la Recherche, France) for its financial support to the project "SOOT" No. ANR-06-BLAN-0349-03 and also Professor M. P. Mengüç (University of Kentucky, Lexington, USA) and his team for the many fruitful discussions.

[1] B. Å. S. Gustafson, *Light Scattering by Nonspherical Particles: Theory, Measurements, and Applications*, edited by M. Mishchenko, J. Hovenier, and L. Travis (Academic, New York, 2000), pp. 367–390.
[2] M. I. Mishchenko, J. Quant. Spectrosc. Radiat. Transf. **101**, 411 (2006).
[3] B. Å. S. Gustafson, J. Quant. Spectrosc. Radiat. Transf. **55**, 663 (1996).
[4] J. M. Geffrin, P. Sabouroux, and C. Eyraud, Inverse Probl. **21**, S117 (2005).
[5] Y. Xu and R. T. Wang, Phys. Rev. E **58**, 3931 (1998).
[6] Y. Xu and B. Å. S. Gustafson, J. Quant. Spectrosc. Radiat. Transf. **70**, 395 (2001).
[7] P. Sabouroux, B. Stout, J. M. Geffrin, C. Eyraud, I. Ayranci, R. Vaillon, and N. Seliçuk, J. Quant. Spectrosc. Radiat. Transf. **103**, 156 (2007).
[8] R. H. Zerull, B. Å. S. Gustafson, K. Schulz, and E. Thiele-Corbach, Appl. Opt. **32**, 4088 (1993).
[9] J. E. Thomas-Osip, B. Å. S. Gustafson, L. Kolokolova, and Y. Xu, Icarus **179**, 511 (2005).
[10] L. Kolokolova and B. Å. S. Gustafson, J. Quant. Spectrosc. Radiat. Transf. **70**, 611 (2001).
[11] C. Eyraud, J. M. Geffrin, P. Sabouroux, P. C. Chaumet, H. Tortel, H. Giovannini, and A. Litman, Radio Sci. **43**, RS4018 (2008).
[12] C. Eyraud, J. M. Geffrin, A. Litman, P. Sabouroux, and H. Giovannini, Appl. Phys. Lett. **89**, 244104 (2006).
[13] I. Ayranci, Ph.D. thesis, Middle-East Technical University, Ankara, Turkey and INSA Lyon, Villeurbanne, France, 2007.
[14] D. W. Mackowski, Appl. Opt. **34**, 3535 (1995).
[15] P. Sabouroux and P. Boschi, Rev. Electr. Electron. **10**, 58 (2005).
[16] G. Bohren and D. Huffman, *Absorption and Scattering of Light by Small Particles* (Wiley, New York, 1983).
[17] J. M. Geffrin and P. Sabouroux, Inverse Probl. **25**, 024001 (2009).
[18] D. W. Mackowski and M. I. Mishchenko, J. Opt. Soc. Am. A **13**, 2266 (1996).